Determination of the physical environment within the *Chlamydia trachomatis* inclusion using ion-selective ratiometric probes

Scott Grieshaber,[1] Joel A. Swanson[2] and
Ted Hackstadt[1]*

[1]*Host-Parasite Interactions Section, Laboratory of
Intracellular Parasites, Rocky Mountain Laboratories,
NIAID, NIH, Hamilton, MT 59840, USA.*
[2]*Department of Microbiology and Immunology,
University of Michigan Medical School, Ann Arbor,
MI 48109-0620, USA*

Summary

Chlamydia trachomatis **is an obligate intracellular
bacterium with a biphasic life cycle that takes place
entirely within a membrane-bound vacuole termed an
inclusion. The chlamydial inclusion is non-fusogenic
with endosomal or lysosomal compartments but
intersects a pathway involved in transport of sphin-
gomyelin from the Golgi apparatus to the plasma
membrane. The physical conditions within the mature
chlamydial inclusion are unknown. We used ratiomet-
ric imaging with membrane-permeant, ion-selective
fluorescent dyes for microanalyis of the physical
environment within the inclusion. Determination of
H^+, Na^+, K^+ and Ca^{2+} concentrations using CFDA
(carboxy fluorescein diacetate) or BCECF-AM
(2′,7′-bis (2-carboxyethyl)-5,6-carboxyfluorescein
acetoxymethyl ester, SBFI-AM, PBFI-AM and fura-
PE3-acetomethoxyester (Fura-PE3-AM), respectively,
indicated that all ions assayed within the lumenal
space of the inclusion approximated the concentra-
tions within the cytoplasm. Stimulation of puringeric
receptors by addition of extracellular ATP triggered a
dynamic Ca^{2+} response that occurred simultaneously
within the cytoplasm and interior of the inclusion. The
chlamydial inclusion thus appears to be freely perme-
able to cytoplasmic ions. These results have implica-
tions for nutrient acquisition by chlamydiae and may
contribute to the non-fusogenicity of the inclusion
with endocytic compartments.**

Introduction

Chlamydia trachomatis is the most common sexually
transmitted disease in developed countries and the
most frequent cause of preventable blindness world-wide
(Schachter *et al.*, 1988). *Chlamydia* spp. are obligate
intracellular bacteria with a unique developmental cycle,
which takes place entirely within a membrane-bound par-
asitophorous vacuole termed an inclusion (Moulder, 1991;
Friis, 1972). The chlamydial developmental cycle is
characterized by two morphologically distinct forms;
elementary bodies (EBs) are the infectious form, and
reticulate bodies (RBs) are the replicative form (Friis,
1972; Moulder, 1991). Infection of host cells is initiated by
EBs. A transition from the EB form to the RB form occurs
within the first few hours after internalization. The RBs
multiply by binary fission until approximately 18 h post
infection (for serovar L2), at which time they begin to
convert back to EBs which accumulate within the inclu-
sion until the cell lyses at 44–48 h post infection.

Intracellular pathogens have developed many means of
survival within eukaryotic cells associated with replication
in different intracellular compartments. Some, such as
members of the genus *Rickettsia,* live freely within the
host cell cytosol and therefore have direct access to nutri-
ents. Other intracellular parasites reside in membrane-
bound vesicles. For example, *Coxiella burnetii* is confined
to a membrane-bound vacuole that displays characteris-
tics of lysosomes and is fusogenic with the endosomal
pathway. In this way, it has access to nutrient-rich vesi-
cles involved in fluid phase uptake or turnover of endoge-
nous cellular components. *Chlamydia* spp., however,
appear not to interact with the endocytic pathway and do
not fuse with endocytic vesicles (Heinzen *et al.*, 1996).
The chlamydial inclusion appears to intersect an exocytic
pathway as it fuses with Golgi-derived sphingomyelin con-
taining vesicles (Hackstadt *et al.*, 1995; 1996). However,
the contents of these vesicles are unknown. Some proto-
zoan parasites, such as *Plasmodium falciparum* (Desai *et
al.*, 1993) and *Toxoplasma gondii* (Schwab *et al.*, 1994),
are confined to vacuoles containing pores that provide
access to many small molecules of less than 1700 Da
from the host cytoplasm. This differs from the chlamydial
inclusion which is impermeable to molecules as small as
520 Da (Heinzen and Hackstadt, 1997).

The fragility of the *C. trachomatis* inclusion has pre-
cluded its purification in an intact form. Indeed, the inclu-
sion membrane is so fragile that the host cells containing
mature vacuoles cannot be microinjected without collaps-

ing the inclusion (Heinzen and Hackstadt, 1997). These technical challenges have prevented definition of the physical conditions within the inclusion by conventional biochemical techniques. Thus, the environment in which chlamydiae carry out their life cycle and the mechanisms by which they obtain nutrients, exchange metabolites, and communicate with the host cell remain unclear.

In this study, we used membrane-permeant ratiometric dyes to determine the ionic conditions within the chlamydial inclusion. The use of ratiometric dyes permits the measurement of ionic concentrations within intact, viable inclusions. By measuring the ratio of the emissions from two different excitation wavelengths, variations in fluorescence intensity due to cell loading and path length are negligible, as they affect both wavelengths equally. Therefore, the ratio differences reflect only the ionic conditions to which the probe is responsive (Negulescu and Machen, 1990). We determined that the *C. trachomatis* inclusion membrane is freely permeable to ions and that the ionic conditions within the mature inclusion are indistinguishable from the cell cytosol.

Results

pH of the Chlamydia trachomatis Inclusion

To determine the pH within both the cell cytoplasm and the chlamydial inclusion, Vero cells infected with *C. trachomatis* L2 were loaded with carboxy fluorescein diacetate (CFDA). The pKa of CFDA makes it suitable for measuring pH near neutrality (Thomas *et al.*, 1979). The fluorescent emissions of CFDA when excited at 440 nm are not affected by pH and are therefore considered the isosbestic point. However, the fluorescence intensity of CFDA when excited at 480 is sensitive to pH, thus the ratio of fluorescence excited at 440 and 480 nm can be calibrated and used to determine pH. To determine the pH in the inclusion and the cell cytoplasm, the ratio values obtained for the separate compartments were plotted against the ratio values subsequently obtained from cells on the same coverslip after treatment with ionophores and equilibration with pH standard buffers. Separate standard curves were used to calculate pH for the chlamydial inclusion and the cell cytoplasm. In the case of CFDA, the standard curves within the cytoplasm and the inclusion overlapped. Figure 1A shows a representative 440 nm, 480 nm, phase-contrast and ratio image. The 440 nm and 480 nm images showed uniform loading and fluorescence of the probe in both the cell cytoplasm and inclusion. The resulting 480/440 ratio images demonstrated nearly uniform ratios in both these compartments. The values calculated for pH were 7.29 ± 0.07 for the cytoplasm and 7.25 ± 0.19 for the inclusion (Fig. 1B).

A second pH-sensitive probe, 2′,7′-bis (2-carboxyethyl)-5,6-carboxyfluorescein acetoxymethyl ester (BCECF-AM)
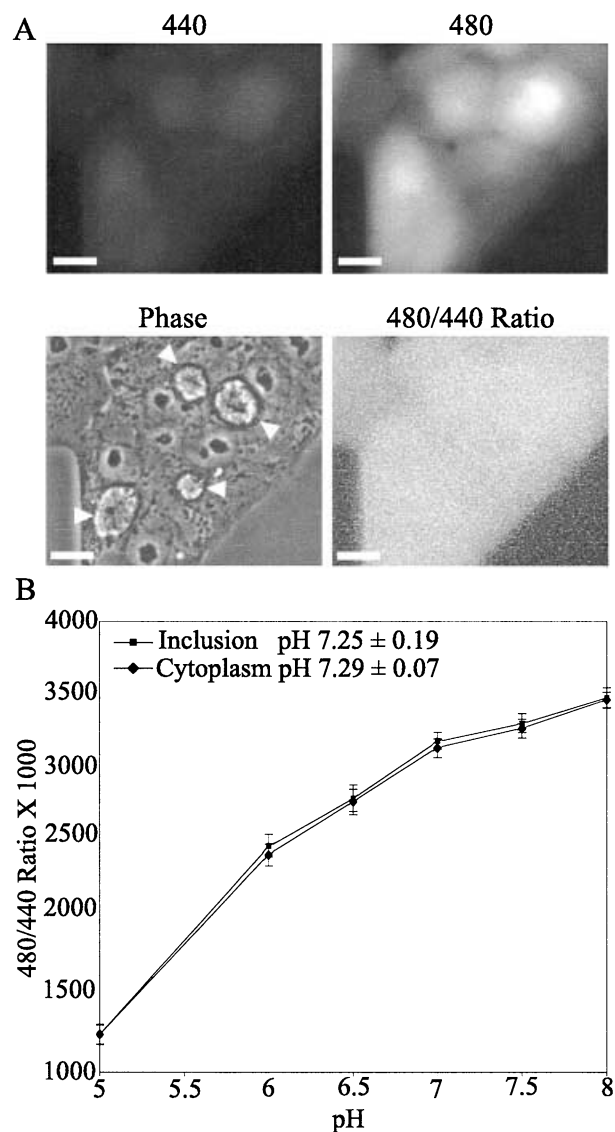

Fig. 1. Determination of the pH in *C. trachomatis* inclusions using ratiometric analysis of CFDA loaded *C. trachomatis* L2 infected Vero cells. Vero cells were infected for 20 h before loading with CFDA-AM.

A. A representative field of infected cells showing fluorescent emissions at 440 and 480 nm excitation frequencies and the corresponding phase-contrast and 480/440 ratio images. Note the similar fluorescent intensity for both the chlamydial inclusions and the Vero cell cytoplasm. Ratio images were generated from five microscopic fields; two to five regions of interest per field within both the cytoplasm and inclusion lumen were defined and quantified. Arrowheads in the phase-contrast image indicate chlamydial inclusions. Bar equals 10 μm.

B. The ratio data were plotted against a standard curve that was generated from five microscopic fields and two to five defined regions of interest within the cytoplasm or inclusion for each of the six pH standards. These curves were used to determine the pH within both the Vero cell cytoplasm and the chlamydial inclusion. The pH for the inclusion was calculated to be 7.29 ± 0.07 (*n* = 12) and for the Vero cell cytoplasm was 7.25 ± 0.19 (*n* = 12).

(Rink *et al*., 1982), was used to verify the results obtained with CFDA. BCECF, like CFDA, has an isosbestic point at 440 nm and pH-sensitive fluorescence when excited at 480 nm (Negulescu and Machen, 1990). Figure 2 shows representative 440 nm, 480 nm, phase-contrast and ratio images. Unlike CFDA, BCECF did not load the infected cells uniformly (Fig. 2A). The probe appeared to concen-
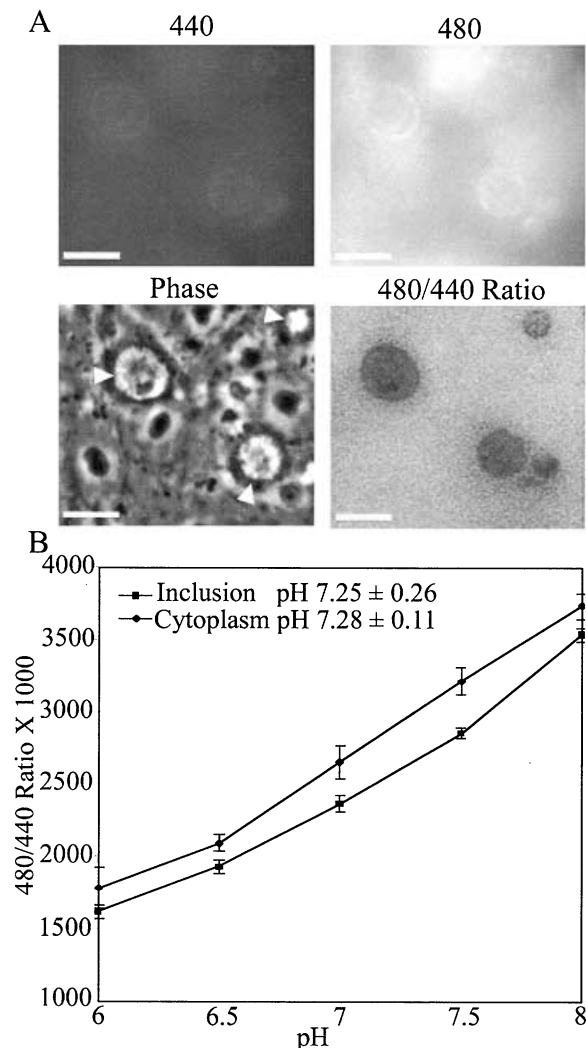

Fig. 2. Determination of pH in *C. trachomatis* inclusions using the pH-sensitive probe BCECF.
A. Representative micrographs of BCECF-AM loaded Vero cells that had been infected with *C. trachomatis* L2 for 20 h shows the fluorescent signal from the dye at both 440 and 480 nm excitation wavelengths and the corresponding phase-contrast and 480/440 ratio images. Arrowheads in the phase-contrast image indicate chlamydial inclusions. Bar equals 10 μm.
B. Separate standard curves were generated for both the inclusion and host cell cytoplasm as described in the legend of Fig. 1. These standard curves parallelled but did not overlap each other indicating that the probes responded similarly to the pH standards in both compartments. The experimental values obtained for these compartments was determined to be pH 7.25 ± 0.26 (*n* = 10) for the chlamydial inclusion and 7.28 ± 0.11 (*n* = 10) for the Vero cell cytoplasm.

trate in the inclusion as compared to the cytoplasm (as can be seen in both the 440 nm and 480 nm images). Because of these loading differences, standard curves were generated independently for both the cytoplasm and inclusion. Experimental results for the two compartments were plotted against the respective standard curve. Although the two standard curves differed in absolute ratio values, the slopes of the curves were the same, indicating that the probe responded equally to the pH standards (Fig. 2B). The results obtained using BCECF were equivalent to those obtained with CFDA, with pH values of 7.28 ± 0.11 for the cytoplasm and 7.25 ± 0.26 for the inclusion.

To confirm the pH within the inclusion lumen without the possible interference by any probe accumulated within RBs, we treated the cells with 100 μg ml^{-1} ampicillin during infection. Ampicillin does not effect the development of the chlamydial inclusion but causes the formation of aberrantly large RB forms and inhibits RB to EB development (Gutter *et al*., 1973; Cevenini *et al*., 1988). These aberrant RBs do not divide but increase in size, leaving large empty regions within the inclusion. These regions are more readily delimited for quantitation, as there is less interference from the RBs. Figure 3A shows representative micrographs of ampicillin-treated infected cells loaded with CFDA. The pH of the inclusion lumen of ampicillin-treated infected cultures was similar to inclusions without ampicillin treatment. The pH of these inclusions was 7.10 ± 0.21, which was in close agreement with the pH of the cytoplasm (7.06 ± 0.20) (Fig. 3B).

To verify the ratiometric techniques in a conventional endocytic vacuole, we used two different probes to determine the pH of the *Coxiella burnetii* vacuole. *Coxiella burnetii* resides in a vacuole that has many of the characteristics of a secondary lysosome (Heinzen *et al*., 1996). The *C. burnetii* vacuole was not accessible to either membrane-permeant BCECF-AM or CFDA (data not shown) but did load with BCECF-free acid or Oregon green dextran via fluid-phase endocytosis. BCECF has a pKa of about 7, rendering it of limited use as a pH-sensitive probe in the acidic range (Paradiso *et al*., 1984). We found this to be true for measuring the pH of the *C. burnetii* vacuole as well. We measured the pH of the BCECF acid-loaded *C. burnetii* vacuole as 6.4 ± 0.2, however the standard curve for this probe indicated a poor response at low pH (data not shown). Oregon green dextran also loaded the *C. burnetii* vacuole well; with a pKa of approx. 4.7, it has spectral properties that respond to low pH better than BCECF (Haugland, 1997). Figure 4A shows a representative phase-contrast image of *C. burnetii* vacuoles and the corresponding ratio image. Ratiometric measurements using this probe gave a pH of 4.88 ± 0.14 for the *C. burnetii* vacuole. The standard curve for Oregon green dextran (Fig. 4B) demonstrated good pH response in this range.
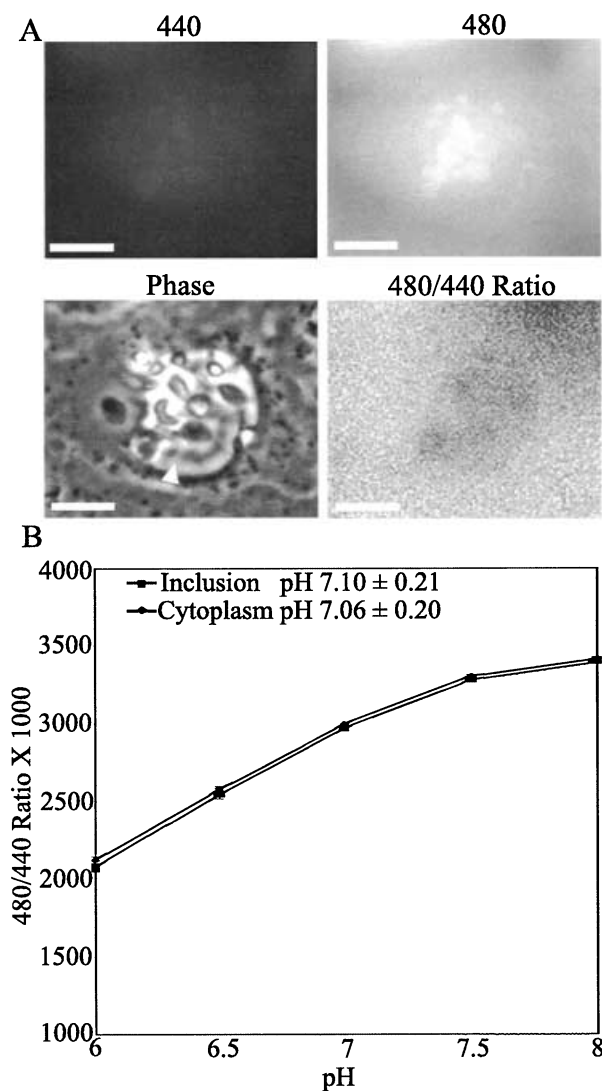
Fig. 3. Treatment with ampicillin improves visualization and analysis of the inclusion lumenal space.
A. Vero cells were infected with *C. trachomatis* for 20 h in the presence of 100 µg ml⁻¹ ampicillin before loading with CFDA. Representative micrograph showing fluorescence at 440 and 480 nm excitation frequencies as well as the phase-contrast and ratio image. The probe appeared to load all compartments and was readily visible in the lumenal space. The phase image shows the aberrant RBs surrounded by large empty regions of lumenal space that were used for analysis. Arrowhead in the phase-contrast image indicates the lumenal space within a chlamydial inclusion. Bar equals 10 µm.
B. The standard curves were generated by measuring the ratio values for the cytoplasm and lumenal space as described in the legend of Fig. 1. Experimental values were plotted against the standard curves and the pH of the host cell cytoplasm and lumenal space were calculated. The pH was 7.06 ± 0.20 (*n* = 20) for the cell cytoplasm and 7.10 ± 0.21 (*n* = 20) for the inclusion.

Concentrations of Na⁺ and K⁺ ions are the same in the cytoplasm and inclusions

We also explored the concentrations of other ions in the inclusion. The concentrations of potassium and sodium

ions within the inclusion and cell cytoplasm were determined using the probes PBFI and SBFI respectively. PBFI is a potassium-sensitive dye that is relatively unaffected by K⁺ ions when excited at 380 nm but is reduced in a [K⁺]-dependent manner when excited at 340 nm (Negulescu and Machen, 1990). PBFI, like BCECF, showed substantial compartmentalization. For this reason, a separate standard curve was generated for the cell cytoplasm as well as the inclusion (Fig. 5A). The standard curve for PBFI, particularly within the inclusion, did not show as dynamic a difference in ratios over the physiological range as did the pH probes; however, the greatest response was observed at the concentrations of K⁺ that would be expected of the cytoplasm. The K⁺ concentration in the cytoplasm was determined to be 146 ± 14 mM and for the inclusion was 148 ± 9 mM,
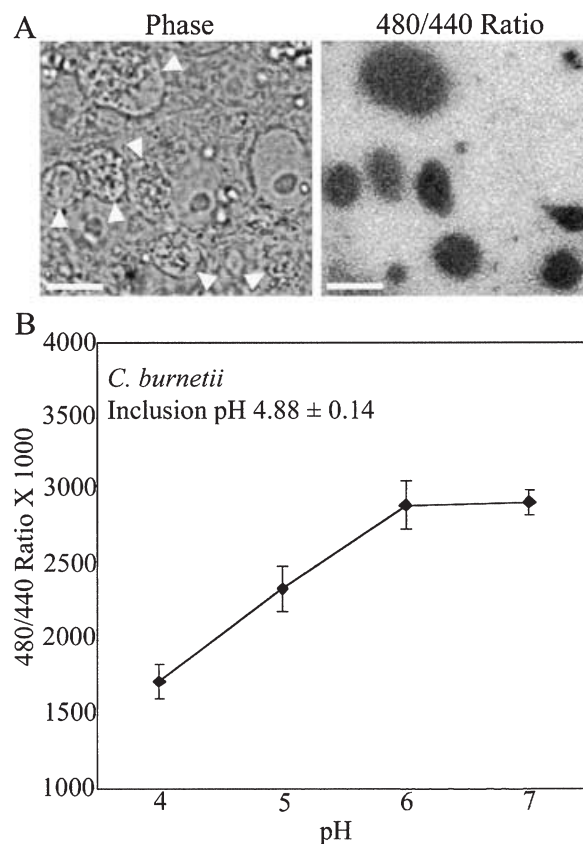

Fig. 4. pH of the *C. burnetii* inclusion in Vero cells. Vero cells were infected with *C. burnetii* 9 mile strain, phase II for 48 h before loading for 20 h with Oregon green dextran.
A. Representative micrographs of Oregon green dextran loaded *C. burnetii* infected Vero cells showing the location of the *C. burnetii* vacuoles seen in the representative phase-contrast image and the corresponding 480/440 ratio image. Arrowheads in the phase-contrast image indicate the *C. burnetii* vacuoles. Bar equals 10 µm.
B. The ratio values were plotted against a standard curve generated as described in the legend to Fig. 1. We determined the pH of *C. burnetii* inclusion to be 4.88 ± 0.14 (*n* = 22).
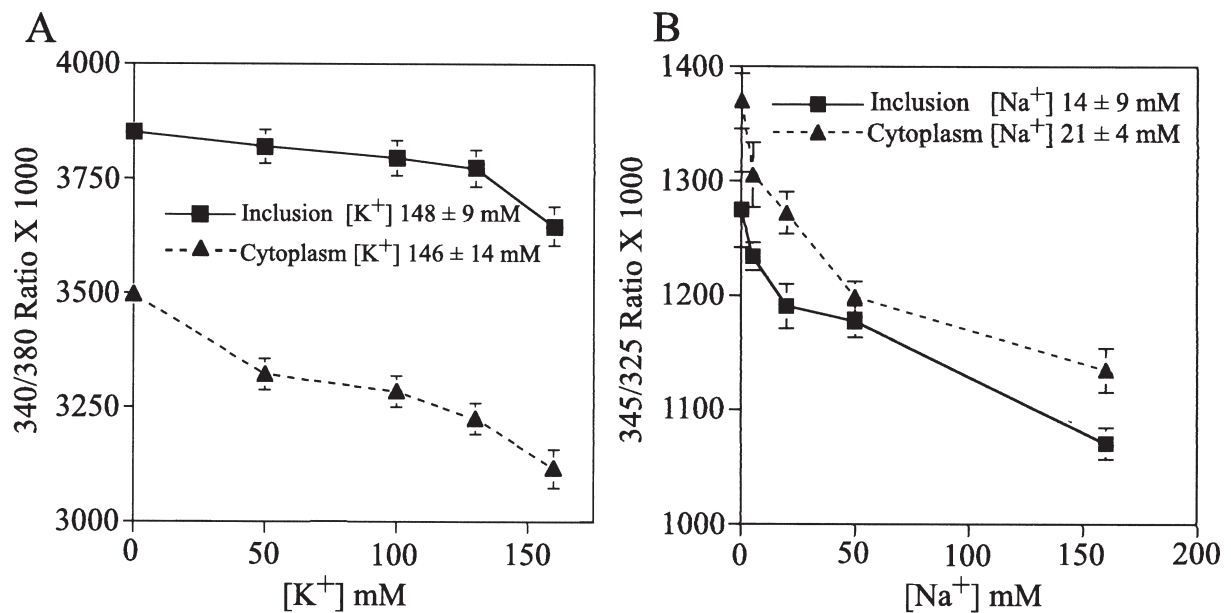
A

B

Fig. 5. The concentrations of Na$^+$ and K$^+$ ions in the chlamydial inclusion were determined using the ratiometric dyes PBFI for K$^+$ (A) and SBFI for Na$^+$ (B). Standard curves were generated independently for the cell cytoplasm and *C. trachomatis* inclusion. The standard curve for PBFI was generated by plotting the 340/380 ratio values obtained with five K$^+$ standards equilibrated with valinomycin. The individual standard curves for the host cell cytoplasm and chlamydial inclusion parallelled each other, indicating the probe responded similarly in both compartments to the potassium standards. The K$^+$ concentration in the host cell cytoplasm was measured as 146 ± 14 mM ($n = 24$) and 148 ± 9 mM ($n = 24$) for the *C. trachomatis* inclusion. The standard curve for SBFI was generated in much the same way as for PBFI. Vero cells were infected with *C. trachomatis* L2 for 20 h in the presence of 100 μg ml^{-1} ampicillin. Ratio values using 345/325 nm excitation were plotted against the Na$^+$ standards that were equilibrated with gramicidin. Plotting the experimental values against this standard curve resulted in values of 14 ± 9 mM ($n = 22$) Na$^+$ for the chlamydial inclusion and 21 ± 4 mM ($n = 22$) for the Vero cell cytoplasm.

indicating that the potassium ion concentration of the inclusion is the same as that of the cell cytoplasm (Fig. 5A).

We used the AM ester derivative of the Na$^+$-sensitive dye SBFI to measure the Na$^+$ concentration in the inclusion. SBFI-AM also showed considerable compartmentalization in infected cells. Multiple attempts to determine the lumenal Na$^+$ concentration within the chlamydial inclusion resulted in values that were similar to those of the cytoplasm but with large variance (data not shown). The difficulty in obtaining reliable standard curves was attributed to the apparent concentration of the probe within chlamydial RBs. Therefore, ampicillin-treated, infected cells were loaded with SBFI-AM for the determination of Na$^+$ concentrations in the inclusion. The signal from the inclusion was sufficiently above background for reliable ratiometric measurements. We first characterized the spectral response of SBFI to Na$^+$ ions in our system over excitation wavelengths of 320–400 nm, in 5 nm steps, under both high Na$^+$ conditions (160 mM) and low Na$^+$ conditions (0 mM). This plot showed that the fluorescent emissions at 345 nm excitation exhibited the highest degree of Na$^+$ sensitivity and the least sensitivity to differences in [Na$^+$] when excited at 325 nm (data not shown). Ratio images were constructed using 325 nm as the isosbestic point and 345 nm for the Na$^+$-sensitive

excitation frequency. Separate standard curves were generated from values measured from the cytoplasm and the inclusion. As with PBFI, the range of ratio values was not large but the greatest differences were observed over the Na$^+$ concentrations expected of the cytoplasm. By plotting the experimental values against the standard curves, the measured [Na$^+$]$_i$ was similar in both the cytoplasm (21 ± 4 mM) and the inclusion (14 ± 9 mM) (Fig. 5B).

Calcium concentration within the inclusion

We also determined the concentrations of free Ca^{2+} in the inclusion as well as the cell cytoplasm, using FURA-PE3 AM. Ratio images were taken and [Ca^{2+}] was calibrated according to published equations, the published value for the K_d of Fura-PE3 (250 nM) (Grynkiewicz *et al.*, 1985; Vorndran *et al.*, 1995), and maximum and minimum values generated experimentally in calcium-free and calcium-saturating conditions in the presence of the calcium ionophore ionomycin. Separate maximum and minimum values were calculated for the cytoplasm and the inclusion. The free Ca^{2+} concentration was determined to be similar in the cytoplasm and chlamydial inclusion with values of 42 ± 3 nM for the cytoplasm and 34 ± 4 nM for the inclusion (Table 1).

Table 1. Ca²⁺ concentration within the *C. trachomatis* inclusion and host cell cytoplasm.

	Inclusion	Cytoplasm
R_{min}	1271.44	1365.24
R_{max}	1595.58	1981.79
Q	1.43	1.76
[Ca²⁺]	34 ± 4 nM	42 ± 3 nM

$[Ca^{2+}] = K_d {*} Q {*} (R-R_{min})/(R_{max}-R)$. $Q = 380_{min}/380_{max}$. $R = 380/340$. K_d (Fura-PE3) = 250 nm.

The inclusion is freely permeable to Ca⁺² ions

To determine if the inclusion was indeed permeable to ions, we used the fact that HeLa cells stimulated with extracellular ATP show a very fast and transient Ca²⁺ increase in the cytoplasm (Paemeleire *et al.*, 2000). This occurs by ATP binding the P2 purinergic receptors on these cells and activating the PLC pathway leading to release of Ca²⁺ stores in the ER lumen (Communi and Boeynaems, 1997; Harden *et al.*, 1997). By observing this transient intracytoplasmic increase in Ca²⁺, we could determine whether the dynamic Ca²⁺ response in the
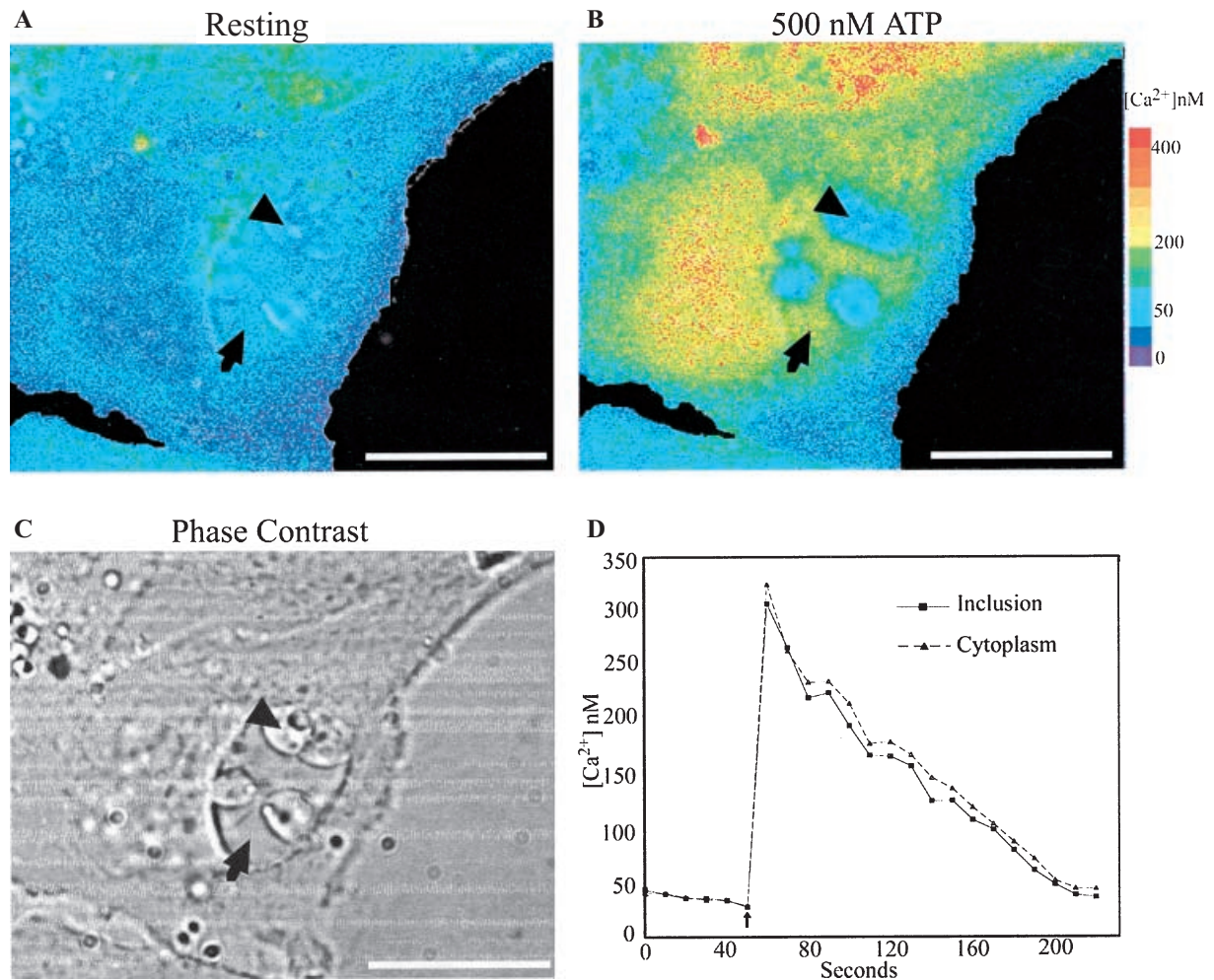

Fig. 6. The *C. trachomatis* inclusion is freely permeable to Ca²⁺ ions. HeLa cells were infected with *C. trachomatis* L2 for 20 h in the presence of 100 μg ml⁻¹ ampicillin.
A–C. The pseudocoloured ratio image shows the Ca²⁺ concentration in these cells before ATP stimulation is low with values of about 45 nM Ca²⁺ in both the cytoplasm and the lumenal space. After addition of HBSS containing 500 mM ATP, the Ca²⁺ concentration in the cell rose dramatically. The pseudocolour image shows the highest levels of Ca²⁺ after ATP addition. This Ca²⁺ peak was of similar magnitude in both the cytoplasm and lumenal space (arrow). This Ca²⁺ spike was not observed in the RBs themselves (arrowhead). The phase-contrast micrograph shows the location of the chlamydial inclusion with the aberrant RBs (arrowhead) and the lumenal space (arrow). The arrowhead also indicates an aberrantly large RB; the arrow identifies an area within the lumen of the inclusion that is free of RBs. Bar equals 10 μm.
D. A plot of the calibrated Ca²⁺ concentrations within a typical cell and inclusion before and after addition of 500 nM ATP shows that, after addition of ATP, the Ca2+ concentration in the cell rises dramatically, then over time (170 s) gradually returns to resting levels. The dynamic Ca²⁺ response was the same for both the cell cytoplasm as for the chlamydial inclusion, indicating Ca²⁺ ions freely diffused into the lumenal space without noticeable delay. This reponse is typical of over eight infected cells observed.
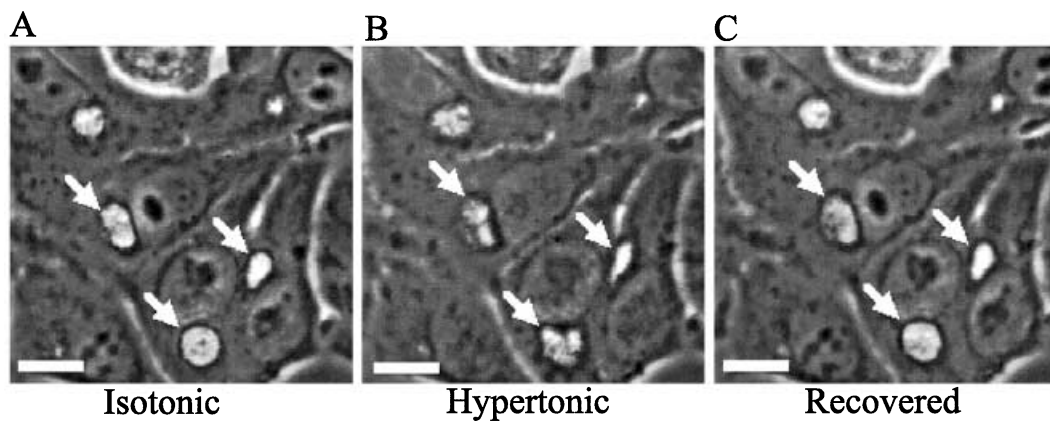
Fig. 7. The swollen shape of *C. trachomatis* inclusion is maintained by osmotic pressure.
A. Vero cells infected with *C. trachomatis* L2 under isotonic conditions in HBSS have inflated, spherical-shaped inclusions.
B. After placing these cells under hypertonic conditions (250 mM sucrose in HBSS) the inclusions became misshapen and less phase bright.
C. When the cells were returned to isotonic conditions, the inclusions returned to their original spherical shape.
A–C. Arrows indicate chlamydial inclusions. Bar equals 10 μm.

cytoplasm was also seen in the inclusion lumen. *Chlamydia trachomatis*-infected HeLa cells were loaded with Fura-PE3-AM in the presence of 100 μg ml^{-1} ampicillin. Ampicillin was included in the media during the infection to allow more ready visualization of the inclusion lumen. Resting values for the lumenal Ca^{2+} were 35 ± 2 nM in the presence of ampicillin, a value similar to that determined above in the absence of antibiotic. Images were acquired every 10 s for 220 s. At the 50-s time point, the medium was aspirated and Hanks' buffered saline solution (HBSS) containing 500 nM ATP was added to the cells. The addition of ATP induced a large calcium spike in the cell cytoplasm within 10 s after addition. This calcium spike extended to the lumenal inclusion space without noticeable delay, peaking at 325 nM Ca^{2+} in both the cell cytoplasm and inclusion (Fig. 6A, arrow). The Ca^{2+} spike was not, however, propagated into the chlamydial RBs (Fig. 6A, arrow head). Calcium concentrations in both the cell and chlamydial inclusion returned to resting levels, about 40 nM, by 210 s. Thus the dynamics of the calcium spike and recovery in the cytoplasm was mimicked in the lumen of the inclusion (Fig. 6B). The experiment was also performed in the absence of ampicillin treatment with similar results (data not shown). A previous study by Majeed *et al*. (1999) showed a similar transient increase in intracellular calcium upon ATP stimulation of *C. trachomatis*-infected cells, although this was considered to be in proximity to the inclusion and did not resolve Ca^{2+} flux within the lumenal space of the inclusion (Majeed *et al.*, 1999).

The chlamydial inclusion shape may be maintained osmotically

Because the ionic conditions within the chlamydial inclusion mimic that of the cell cytoplasm, we examined the effects of osmolarity on the swollen nature of the L2 inclusion. Time-lapse, phase-contrast images of *C. trachomatis* L2-infected cells were taken every 5 s for 2 min. Images were recorded for 30 s in isotonic conditions (HBSS) before being placed under hypertonic conditions (HBSS + 250 mM sucrose). Under isotonic conditions the *C. trachomatis* inclusion generally appeared as a spherical structure with a spacious, fluid-filled centre (Fig. 7A, arrows). Within 5 s under hypertonic conditions, the chlamydial inclusions appeared compacted and misshapen (Fig. 7B, arrows). When the cells were returned to isotonic conditions (HBSS), the chlamydial inclusions returned to near normal shape within 30 s (Fig. 7C arrows). This suggests that the shape and swollen nature of the chlamydial inclusion may be maintained by osmotic pressure.

Discussion

The physical conditions within the parasitophorous vacuoles occupied by intracellular parasites are largely unknown. Determination of intravacuolar ionic concentrations within these specialized compartments is not amenable to methods that require purification of the organelle for analysis as leakage of the contents during purification or contributions of the parasites themselves could confound assays. Standard techniques such as atomic adsorption spectroscopy, radioisotopic distribution or ion-selective probes are therefore not possible. The inability to assay selectively specific intracellular compartments within viable intact cells further precludes these techniques. The temporal and spatial resolution of ratiometric imaging using dyes whose emissions are responsive to the concentrations of specific ions permits

Table 2. Summary of the ionic conditions within the *C. trachomatis* inclusion.

Ion	Inclusion	Cytoplasm
pH (CFDA)	7.25 ± 0.19	7.29 ± 0.07
pH (BCECF)	7.25 ± 0.26	7.28 ± 0.11
K^+	$148 \pm 9\,mM$	$146 \pm 14\,mM$
Na^+	$14 \pm 9\,mM$	$21 \pm 4\,mM$
Ca^{2+} (resting)	$34 \pm 4\,n\text{M}$	$42 \pm 3\,n\text{M}$

microanalysis of intracellular compartments within living cells. Ratiometric probes were therefore used to estimate the ionic conditions within the lumenal space of the mature *C. trachomatis* inclusion. Determinations of H^+, Na^+, K^+ and Ca^{2+} concentrations (Table 2) indicated that each of these ions approximated concentrations within the cytoplasm. Moreover, induction of a Ca^{2+} pulse by stimulation of purinergic receptors revealed that Ca^{2+} concentrations within the inclusion paralleled that of the cytoplasm. The results indicate that the chlamydial inclusion membrane is freely permeable to small ions.

We had previously reported that the chlamydial inclusion membrane was impermeable to fluorescent molecules as small as 520 Da after microinjection of the probes into the cytoplasm of infected cells (Heinzen and Hackstadt, 1997). Because Ca^{2+}, with an atomic mass of 45 Da, is freely permeable across the inclusion membrane, the collective results suggest a pore size of between 45 and 520 Da. Fluorescent probes of less than 500 Da that are suitable for microinjection are not readily available, thus refinement of the molecular weight cut-off for exclusion is not currently possible. Based upon the impermeability of small fluors in microinjection experiments (Heinzen and Hackstadt, 1997), it was concluded that the chlamydial inclusion membrane differed from the parasitophorous vacuole membrane of *Toxoplasma gondii*, which is freely permeable to probes of less than 1700 Da in size (Schwab *et al.*, 1994). Although the pore size differs, it now appears that the parasitophorous vacuolar membranes of both of these very different intracellular parasites allow free diffusion of small molecules but exclude larger molecules. While this would presumably permit ready access to soluble host precursors, a fundamental question is why it might be advantageous to parasites to create such a semiporous membrane to sequester themselves rather than occupying the cytoplasm, which should also provide them with free access to host nutrients. One possibility is avoidance of potentially bacteriocidal macromolecules, for example proteins, in the cytoplasm while maintaining free access to the nutrient-rich cytoplasm. Alternatively, the function of the semiporous membrane may not be to exclude host macromolecules but to prevent the release of parasite

proteins or peptides that could serve as substrates for immune presentation. A final consideration is that the absence of an electrochemical gradient across the inclusion membrane may play a role in the avoidance of lysosomal fusion that is characteristic of both viable chlamydial inclusions and *T. gondii* parasitophorous vacuoles. Treatment of cells with agents such as lysosomotropic amines or inhibitors of the vacuolar $H \pm$ ATPase, that raise the pH of lysosomes and endosomes, inhibits lysosomal fusion (Hart *et al.*, 1983). It is possible therefore that elimination of an electrochemical gradient across the inclusion membrane may be a factor in the restricted fusogenicity of the inclusion with endosomal compartments.

A common means of loading cellular compartments for ratiometric imaging is by fluid-phase endocytosis of the appropriate ratiometric dye coupled to dextran. The non-fusogenicity of the chlamydial inclusion with endocytic compartments had precluded this approach. Schramm and Wyrick circumvented this problem by direct coupling of the pH-sensitive probe SNAFL to EBs (Schramm *et al.*, 1996). These experiments indicated that the pH of early EB-containing endosomes experienced a transient mild acidification to approximately pH 6.26 at 4 h post infection but then recovered with an increase to about pH 6.60 by 12 h post infection. Because the probe was covalently attached to input EBs, growth and replication of the chlamydiae resulted in diminished signal at time points later than 12 h such that the lumenal pH could not be measured at later times. *Chlamydia trachomatis* L2 does not initiate cell division until approximately 12 h post infection (Shaw *et al.*, 2000), thus a visible lumenal space is not present during this time frame. Another limitation of direct coupling the fluorescent probe to the bacterium is the inability to simultaneously monitor the pH within the vacuole and the cytoplasm. Using membrane-permeant ratiometric probes, we were able to measure the conditions within the lumenal space of the mature *C. trachomatis* inclusion and compare that to the host cytoplasm. The two different experimental approaches, while complementary, do not, however, provide a means for a single probe to analyse the entire developmental cycle because the close approximation of the inclusion membrane with the nascent RBs does not leave sufficient fluid space to load and visualize using membrane-permeant probes.

The distortion and shrinkage of the inclusion by incubation in hypertonic sucrose solutions suggests that the turgid structure of the inclusion may be maintained by osmotic pressure in the apparent absence of an actively maintained electrochemical gradient across the inclusion membrane. Although these experiments confirm the porosity of the inclusion membrane by demonstrating

water efflux, it is somewhat difficult to reconcile an osmotic mechanism with the porosity of the inclusion membrane, particularly until the precise pore size is determined. For osmotic activity to play a role, a high molarity of some small solute must be present. Mono- or disaccharides in equilibrium with the glycogen present in the *C. trachomatis* inclusion might be a possibility but until an accurate molecular weight cut-off is determined, the identity and role of any osmotic agent must remain speculative.

Coxiella burnetii, a bacterial obligate intracellular parasite that replicates within a vacuole displaying lysosomal markers (Heinzen *et al.*, 1996), was used as a control for the intravacuolar pH determinations. Direct comparison of *C. trachomatis* and *C. burnetii* vacuoles was not possible for several reasons. The most accurate determinations of pH using ratiometric dyes are within one pH unit of the pKa of the probe (Negulescu and Machen, 1990). Because *C. trachomatis* replicates within a neutral compartment and *C. burnetii* in an acidic compartment, no single probe was appropriate for both. Furthermore, it was not possible to load the distinct compartments with the same probe. Several determinations of the *C. burnetii* intravacuolar pH have been published. These values range from 5.21 ± 0.07 (Akporiaye *et al.*, 1983) to 4.42–5.08 (Maurin *et al.*, 1992) using FITC-dextran as a reporter and 5.82 ± 0.12 using directly coupled SNAFL (Schramm *et al.*, 1996). Because the pKa of these probes, 6.4 for FITC and 7.8 for SNAFL (Whitaker *et al.*, 1991; Zhou *et al.*, 1995), is in a range that is marginal for determination of lysosomal pH, we used Oregon green dextran, with a pKa of 4.7 to measure a pH of 4.88 ± 0.14 in *C. burnetii*-containing vacuoles. This value closely matches the optimum pH for metabolism by *C. burnetii* (Hackstadt and Williams, 1981) and corresponds to that of mature lysosomes (Maxfield, 1989).

Most cellular organelles actively maintain electrochemical gradients across their membranes. We had previously speculated that the chlamydial inclusion might also maintain a electrochemical gradient that could be coupled to nutrient acquisition or maintenance of inclusion structure. The equilibration of H^+, Na^+, K^+ and Ca^{2+} makes it unlikely that an electrical potential across the inclusion membrane exists to be coupled to any bioenergetic function. Chlamydiae obtain many precursors, such as amino acids, glycolytic or tricarboxylic acid cycle substrates, and nucleosides, from the host cell. How these are acquired across the inclusion membrane has been a significant question in chlamydial biology. Because the molecular masses of these precursors are in the range of approximately 100–300 Da, they fall within a range that does not permit ready determination whether they are delivered to the lumen of the inclusion via simple diffusion or require a more active transport process. Simple diffusion through the inclusion membrane now appears to be a likely mechanism by which some small molecules may enter the lumen of the inclusion where they would then be available to chlamydial amino acid, sugar, nucleotide or other transporters. Further studies of the inclusion membrane properties will be necessary to establish which precursors might enter by this means or require facilitated delivery across the inclusion membrane.

Experimental procedures

Organisms, infection and cell culture

Chlamydia trachomatis, LGV 434, serotype L2 was cultivated in HeLa 229 [CCL-2.1: American Type Culture Collection (ATCC)] and Vero (African green monkey kidney cells, ATCC) cells as described previously (Heinzen *et al.*, 1996). *Coxiella burnetii* Nine Mile strain in phase II was propagated in Vero cells. EBs used for infections were purified by Renografin (E. R. Squibb and Sons, Princeton, NJ) density gradient centrifugation (Caldwell *et al.*, 1981).

Vero or HeLa cells were seeded on 25 mm #1 borosilicate coverslip slides (Life Science Products) at a density of 3×10^5 cells per coverslip and cultivated overnight at 37°C in RPMI medium (Invitrogen, Carlsbad, CA) supplemented with 10% fetal bovine serum (FBS) (Invitrogen) and $10 \, \mu g \, ml^{-1}$ gentamicin (Invitrogen) under 5% CO_2. Monolayers at approximately 60–80% confluency were infected with *C. trachomatis* at a multiplicity of infection (MOI) of approximately 1. After 1 h, the inoculum was removed and replaced with RPMI media containing 10% FBS and $10 \, \mu g \, ml^{-1}$ gentamicin. Infections were allowed to proceed for 20–24 h before dye loading and imaging.

Microscopy and image acquisition

Images were recorded on a digital imaging system consisting of an inverted Nikon Eclipse TE300 microscope, a Polychrome I polychromatic illumination system (Applied Scientific Instrumentation, Eugene, OR) and a Princeton Systems Micromax digital camera (Princeton, NJ) under computer control of MetaMorph software (Universal Imaging, Boston, MA). A 520 nm barrier filter was in the lightpath for the collection of paired images after illumination at two different excitation wavelengths corresponding to those most and least responsive to changes in concentration of the ion recognized by the particular fluorescent probe used (see below). A phase-contrast image of the field of view was also taken. Ratio images were created by dividing the individual pixel values of the paired raw images using the program IMAGEJ (written by Wayne Rasband at the US National Institutes of Health and available by anonymous FTP from http://rsb.info.nih.gov/ij/). Regions of interest encompassing approximately 285 pixels were defined in the phase-contrast image and were superimposed onto the ratio image to quantify the ratio values. A minimum of two measurements each were taken for the lumen of the inclusion and the cytoplasm from each image. At least five images were analysed in the ratio images and average ratio values for the region were used for both calibration and ion measurements. Figures for publication were assembled using ADOBE PHOTOSHOP 6.01 (Adobe Systems).

pH measurements

The fluorescent probes carboxy fluorescein diacetate (CFDA) and 2′,7′-bis (2-carboxyethyl)-5,6-carboxyfluorescein acetoxymethyl ester (BCECF-AM) were purchased from Molecular Probes (Eugene, OR) and were used independently to load and measure pH in infected cells. *Chlamydia trachomatis*-infected Vero cells were incubated in 10 μM BCECF-AM or 1 μM CFDA dissolved in anhydrous dimethyl sulphoxide (DMSO) and diluted to the final concentration in HBSS without phenol red for 1 h at 37°C. The cells were washed twice with HBSS without phenol red and incubated for 30 min at room temp to allow the dyes to undergo complete conversion to their membrane-impermeant forms. Images for ratiometric calculations were acquired at excitation wavelengths of 440 nm and 480 nm with a fixed emission wavelength of 520 nm. Standard curves were generated with the same coverslips used to produce the experimental images. To generate the standard curves, coverslips were incubated with 10 μM nigericin and 10 μM valinomycin in the pH 6.0 calibration buffer (130 mM KCl, 30 mM NaCl, 10 mM Hepes). The coverslips were subsequently incubated for 10 min in pH calibration buffers adjusted to pH of 4.0, 5.0, 6.0, 6.5, 7.0, 7.5 or 8.0 with *N*-methylgluconate (NMG) base. Ratio images were generated and values for the standard curves were determined by measuring the average ratio value within a region of interest chosen in either the cell cytoplasm or the *C. trachomatis* inclusion. BCECF-free acid and Oregon green dextran 10 000 MW were also purchased from Molecular Probes and used to load *C. burnetii*-infected cells at a concentration of 1 mg ml^{-1} in culture medium overnight (Steinberg and Swanson, 1994). In the case of *C. burnetii*-infected cells, only values for the vacuole were calculated as the fluid-phase probes did not enter the cytoplasm.

Na$^+$ and K$^+$ measurements

The fluorescent probes SBFI and PBFI (Molecular Probes, Eugene OR) were used to measure Na$^+$ and K$^+$ ion concentrations respectively (Negulescu and Machen, 1990). SBFI-AM and PBFI-AM stock solutions, 10 mM in anhydrous DMSO, were diluted 1:1 with 25% w/v Pluronic F-127 immediately before dilution in HBSS without phenol red for cell loading. The final concentration of the probes for loading was 15 μM. Infected cells were loaded for 3 h at 37°C, rinsed twice and incubated in HBSS without phenol red to allow for complete conversion of the AM dyes to their membrane impermeant forms. PBFI-loaded samples were alternately excited at 340 nm and 380 nm, and SBFI-loaded samples were excited alternately at 325 nm and 345 nm Standard curves were constructed by incubating infected monolayers with buffers of known ionic conditions. A high sodium buffer (130 mM sodium gluconate, 30 mM NaCl, 10 mM Hepes, 1 mM CaCl$_2$, 1 mM MgSO$_4$, pH 7.1 with NMG base) and sodium-free buffer (130 mM potassium gluconate, 30 mM KCl, 10 mM Hep es, 1 mM CaCl$_2$, 1 mM MgSO$_4$, pH 7.1 with NMG base) were mixed in various ratios to create a series of standards for generating standard curves for Na$^+$ and K$^+$. Five standards were used for the sodium standard curve: 0 mM Na$^+$, 5 mM Na$^+$, 20 mM Na$^+$, 50 mM Na$^+$ and 160 mM Na$^+$, and five for the potassium standard curve: 0 mM K$^+$, 50, mM K$^+$, 100 mM K$^+$, 130 mM K$^+$ and 160 mM K$^+$. For SBFI and the sodium standards, the coverslips were incubated with 10 μM gramicidin, a Na$^+$ ionophore, and for PBFI and the potassium standards, coverslips were incubated with 10 μM

valinomycin, a K$^+$ ionophore. Regions of interest were chosen within the cell cytoplasm and chlamydial inclusion for both experimental images and standards and average ratio values were calculated.

Ca^{2+} measurements and mobilization

For determination of intracellular calcium, *C. trachomatis* L2-infected cells were incubated in 5 μM fura-PE3-acetomethoxyester (Fura-PE3 AM) in HBSS without phenol red for 1 h at 37°C. Cells were washed twice in HBSS without phenol red and then incubated in the same media for at least 30 min to allow for complete de-esterification of Fura-PE3 AM to the Ca^{2+}-sensitive fluorescent indicator Fura-PE3. Ratio images were taken from five separate fields from infected coverslips excited alternately at 340 nm and 380 nm. Calibration was performed on the same coverslips as the experimental images. Calibration was done according to: $[Ca^{2+}]_i = K_d*Q*(R–R_{min})/(R_{max}–R)$; where K_d = 250 nM, R_{min} = ratio value obtained in Ca^{2+}-free buffer (130 mM KCl, 30 mM NaCl, 10 mM Hepes, 2 mM EGTA, pH 7.1) with 10 μM ionomycin, R_{max} = ratio obtained in HBSS with 10 μM ionomycin, and Q = 380 nm values in Ca^{2+}-free conditions/ 380 nm values in saturating Ca^{2+} (Grynkiewicz *et al.*, 1985; Vorndran *et al.*, 1995).

References

Akporiaye, E.T., Rowatt, J.D., Aragon, A.A., and Baca, O.G. (1983) Lysosomal response of a murine macrophage-like cell line persistently infected with *Coxiella burnetii*. *Infect Immun* **40:** 1155–1162.

Caldwell, H.D., Kromhout, J., and Schachter, J. (1981) Purification and partial characterization of the major outer membrane protein of *Chlamydia trachomatis*. *Infect Immun* **31:** 1161–1176.

Cevenini, R., Donati, M., and La Placa, M. (1988) Effects of penicillin on the synthesis of membrane proteins of *Chlamydia trachomatis* LGV2 serotype. *FEMS Microbiol Lett* **56:** 41–46.

Communi, D., and Boeynaems, J.M. (1997) Receptors responsive to extracellular pyrimidine nucleotides. *Trends Pharmacol Sci* **18:** 83–86.

Desai, S.A., Krogstad, D.J., and McCleskey, E.W. (1993) A nutrient-permeable channel on the intraerythrocytic malaria parasite. *Nature* **362:** 643–646.

Friis, R.R. (1972) Interaction of L cells and *Chlamydia psittaci*: entry of the parasite and host responses to its development. *J Bacteriol* **110:** 706–721.

Grynkiewicz, G., Poenie, M., and Tsien, R.Y. (1985) A new generation of Ca^{2+} indicators with greatly improved fluorescence properties. *J Biol Chem* **260:** 3440–3450.

Gutter, B., Asher, Y., Cohen, Y., and Becker, Y. (1973) Studies on the developmental cycle of *Chlamydia trachomatis:* isolation and characterization of the initial bodies. *J Bacteriol* **115:** 691–702.

Hackstadt, T., and Williams, J.C. (1981) Biochemical stratagem

for obligate parasitism of eukaryotic cells by *Coxiella burnetii*. *Proc Natl Acad Sci USA* **78:** 3240–3244.

Hackstadt, T., Scidmore, M.A., and Rockey, D.D. (1995) Lipid metabolism in *Chlamydia trachomatis*-infected cells: directed trafficking of Golgi-derived sphingolipids to the chlamydial inclusion. *Proc Natl Acad Sci USA* **92:** 4877–4881.

Hackstadt, T., Rockey, D.D., Heinzen, R.A., and Scidmore, M.A. (1996) *Chlamydia trachomatis* interrupts an exocytic pathway to acquire endogenously synthesized sphingomyelin in transit from the Golgi apparatus to the plasma membrane. *EMBO J* **15:** 964–977.

Harden, T.K., Lazarowski, E.R., and Boucher, R.C. (1997) Release, metabolism and interconversion of adenine and uridine nucleotides: implications for G protein-coupled P2 receptor agonist selectivity. *Trends Pharmacol Sci* **18:** 43–46.

Hart, P.D., Young, M.R., Jordan, M.M., Perkins, W.J., and Geisow, M.J. (1983) Chemical inhibitors of phagosome-lysosome fusion in cultured macrophages also inhibit saltatory lysosomal movements. A combined microscopic and computer study. *J Exp Med* **158:** 477–492.

Haugland, R.P. (1997) Synthesis of Fluorinated Fluoresceins. *J Org Chem* **62:** 6469–6475.

Heinzen, R.A., and Hackstadt, T. (1997) The *Chlamydia trachomatis* parasitophorous vacuolar membrane is not passively permeable to low-molecular-weight compounds. *Infect Immun* **65:** 1088–1094.

Heinzen, R.A., Scidmore, M.A., Rockey, D.D., and Hackstadt, T. (1996) Differential interaction with endocytic and exocytic pathways distinguish parasitophorous vacuoles of *Coxiella burnetii* and *Chlamydia trachomatis*. *Infect Immun* **64:** 796–809.

Majeed, M., Krause, K.H., Clark, R.A., Kihlstrom, E., and Stendahl, O. (1999) Localization of intracellular Ca^{2+} stores in HeLa cells during infection with *Chlamydia trachomatis*. *J Cell Sci* **112:** 35–44.

Maurin, M., Benoliel, A.M., Bongrand, P., and Raoult, D. (1992) Phagolysosomes of *Coxiella burnetii*-infected cell lines maintain an acidic pH during persistent infection. *Infect Immun* **60:** 5013–5016.

Maxfield, F.R. (1989) Measurement of vacuolar pH and cytoplasmic calcium in living cells using fluorescence microscopy. *Meth Enzymol* **173:** 745–771.

Moulder, J.W. (1991) Interaction of chlamydiae and host cells in vitro. *Microbiol Rev* **55:** 143–190.

Negulescu, P.A., and Machen, T.E. (1990) Intracellular ion activities and membrane transport in parietal cells measured with fluorescent dyes. *Meth Enzymol* **192:** 38–81.

Paemeleire, K., Martin, P.E., Coleman, S.L., Fogarty, K.E., Carrington, W.A., Leybaert, L., *et al.* (2000) Intercellular calcium waves in HeLa cells expressing GFP-labeled connexin 43, 32, or 26. *Mol Biol Cell* **11:** 1815–1827.

Paradiso, A.M., Tsien, R.Y., and Machen, T.E. (1984) Na^+-H^+ exchange in gastric glands as measured with a cytoplasmic-trapped, fluorescent pH indicator. *Proc Natl Acad Sci USA* **81:** 7436–7440.

Rink, T.J., Tsien, R.Y., and Pozzan, T. (1982) Cytoplasmic pH and free Mg^{2+} in lymphocytes. *J Cell Biol* **95:** 189–196.

Schachter, J., Moncada, J., Dawson, C.R., Sheppard, J., Courtright, P., Said, M.E. *et al.* (1988) Nonculture methods for diagnosing chlamydial infection in patients with trachoma: a clue to the pathogenesis of the disease? *J Infect Dis* **158:** 1347–1352.

Schramm, N., Bagnell, C.R., and Wyrick, P.B. (1996) Vesicles containing *Chlamydia trachomatis* serovar L2 remain above pH 6 within HEC-1B cells. *Infect Immun* **64:** 1208–1214.

Schwab, J.C., Beckers, C.J.M., and Joiner, K.A. (1994) The parasitophorous vacuole membrane surrounding intracellular *Toxoplasma gondii* functions as a molecular sieve. *Proc Natl Acad Sci USA* **91:** 509–513.

Shaw, E.I., Dooley, C.A., Fischer, E.R., Scidmore, M.A., Fields, K.A., and Hackstadt, T. (2000) Three temporal classes of gene expression during the Chlamydia trachomatis developmental cycle. *Mol Microbiol* **37:** 913–925.

Steinberg, T.H., and Swanson, J.A. (1994) Measurement of Phagosome-Lysosome Fusion and Phagosomal pH. *Methods Enzymol* **236:** 147–160.

Thomas, J.A., Buchsbaum, R.N., Zimniak, A., and Racker, E. (1979) Intracellular pH measurements in Ehrlich ascites tumor cells utilizing spectroscopic probes generated in situ. *Biochemistry* **18:** 2210–2218.

Vorndran, C., Minta, A., and Poenie, M. (1995) New fluorescent calcium indicators designed for cytosolic retention or measuring calcium near membranes. *Biophys J* **69:** 2112–2124.

Whitaker, J.E., Haugland, R.P., and Prendergast, F.G. (1991) Spectral and photophysical studies of benzo[c]xanthene dyes: dual emission pH sensors. *Anal Biochem* **194:** 330–344.

Zhou, Y., Marcus, E.M., Haugland, R.P., and Opas, M. (1995) Use of a new fluorescent probe, seminaphthofluorescein-calcein, for determination of intracellular pH by simultaneous dual-emission imaging laser scanning confocal microscopy. *J Cell Physiol* **164:** 9–16.